

REVIEW ARTICLE

Open Access



Iron-based smart alloys for critical applications: a review on processing, properties, phase transformations, and current trends

S. Santosh^{1*}  and M. Pavithran¹

Abstract

On account of their unique shape memory effect (SME), pseudoelasticity, and biomedical applications, shape memory alloys (SMAs) have gained significant acceptance in the industrial trade and biomedical applications over the past few decades. Due to their affordable constituent parts and the availability of large-scale methods that are commonly employed for the manufacturing of stainless steels, Fe-based shape memory alloys offer benefits in commercial production, owing to their low cost compared to NiTi. The increasing insistence on stronger, lighter, and more functional materials paved the way for active materials. SMAs are a distinct grade of active materials. They exhibit attractive attributes like the potential to provide considerable recoverable strain while mechanical loading (superelasticity), shape recovery during heating (shape memory effect), and biocompatibility, which ultimately prove them to be one of the appropriate actuators for applications in the biomedical industry. This paper gives a review of the Martensitic transformation of some of the compositions of Fe-based SMAs, their potential to be used in civil structures as strengthening materials, their applications, and future research needs. This paper also focuses on the application of iron-based SMAs in different fields and the necessity to work on this SMA in the future since results show that Fe-based SMAs have shown good potential and can serve as an apt alternative to Ni-based shape memory alloys, which on the other hand has quite a lot of disadvantages, the key one being costly. Fe-based SMAs are comparatively lower in cost and have a greater scope to work with in the near future.

Keywords Fe-based, Shape memory alloys, Superelasticity, Shape memory effect, Applications

Introduction

Shape Memory Alloys (often called SMA) are a group of metal alloys that have the ability to “remember” their original form. When the metals are twisted or disturbed from their initial shape, they have the ability to come back to their original form when deformed due to external factors such as magnetic field, heat, or stress. The reversible phase transition that SMAs go through, known as the martensitic transformation, causes the SME.

Changes in the action of forces or temperature can cause the martensitic transition. The martensitic transformation, also known as forward transformation, occurs when the austenite phase (high-temperature phase) is cooled which is when the martensite phase appears (low-temperature phase). The widely used applications of shape memory alloys are that connectors for hydraulic tubing in airplanes, heat engines, active vibration control of structures, orthodontic wires, and automatic switches in home devices. Because of the interesting shape memory property, they have found applications in biomedical implants (stents, heart valve tools), Dentistry (orthodontics), MEMS, sensors, actuators, and antennae. Fe-based SMAs, particularly Fe–Mn–Si alloys, exhibit a lot of potential in civil engineering applications, although they

*Correspondence:

S. Santosh
santoshs@ssn.edu.in

¹ Department of Mechanical Engineering, Sri Sivasubramaniya Nadar (SSN) College of Engineering, Kalavakkam, Chennai 603110, India

are still in the early stages of development. So far, the research done on Fe-based SMAs year-wise, source-wise, and country-wise has been depicted in Figs. 1, 2, and 3 respectively. Figure 4a, b represents the shape memory effect and superelasticity in shape memory alloys. Recent advancements in alloy combination and manufacture pave the way for new applications, particularly in the field of fixing and building new constructions, when these SMAs are used as prestressing tendons. These might also serve as a suitable replacement for Ni-based shape memory alloys which are currently being utilized in several fields. Figure 5 gives a brief outlook on shape memory alloy, their properties, and applications.

Few alloy combinations have effectively been investigated and created until now, for example, Ni–Ti–Zr,

Ni–Mn, and Ni–Ti–Pd. Some functional issues actually stay inexplicable in the above alloy combinations. For example, Ni–Al composites are viewed as temperamental; Ni–Ti–Zr and Ni–Mn amalgams are considered to be excessively fragile. This urged us to work on an alternative. A new market for Fe-based SMAs was gradually explored in the 2000s. This market included commodities for which Ni–Ti alloys are fruitless as production components. Large-diameter connecting pipelines for tunnel establishment and crane rail joint bars (fishplates) are the most recent examples that have aided the Fe-based SMAs in breaking into this new industry. In fact, the Fe–Mn–Si SMAs have inherited many of the structural properties associated with stainless steel. Fe–SMAs behavior in corrosive environments (Lee et al. 2016; Michels et al. 2018;

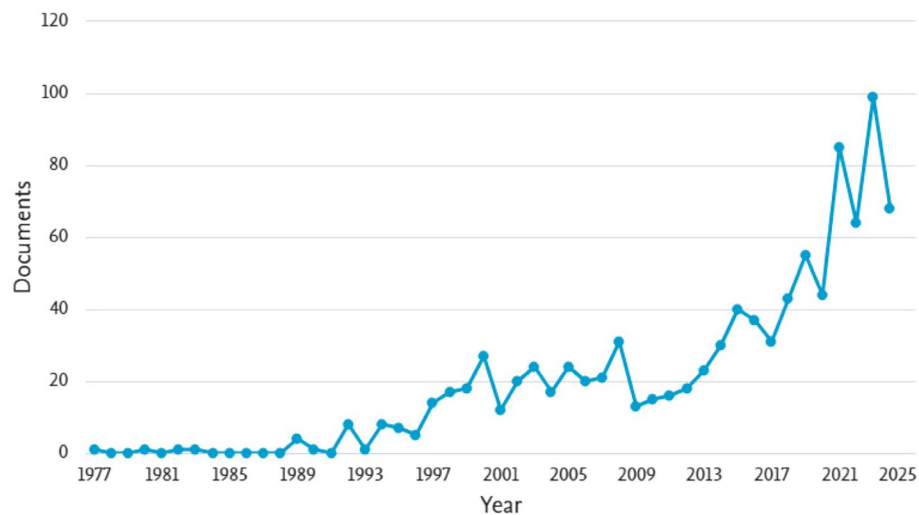


Fig. 1 Documents published on Fe–SMA year-wise (Reference: Scopus database)

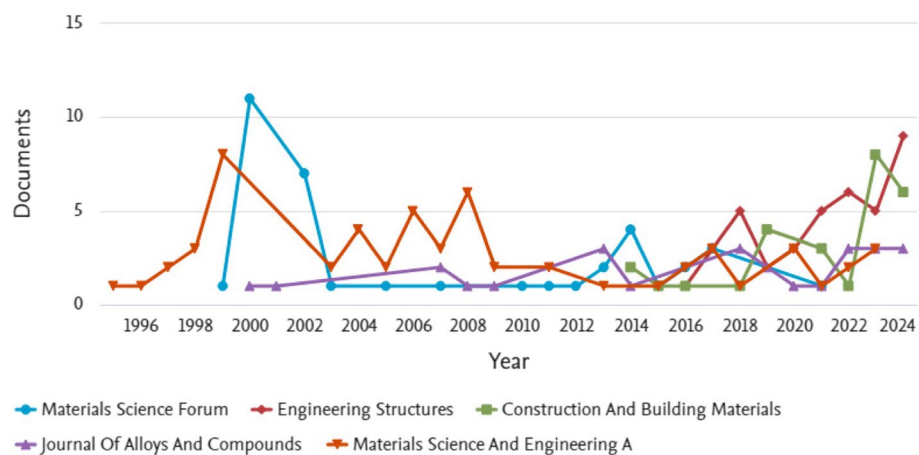


Fig. 2 Documents published on Fe–SMA source-wise (Reference: Scopus database)

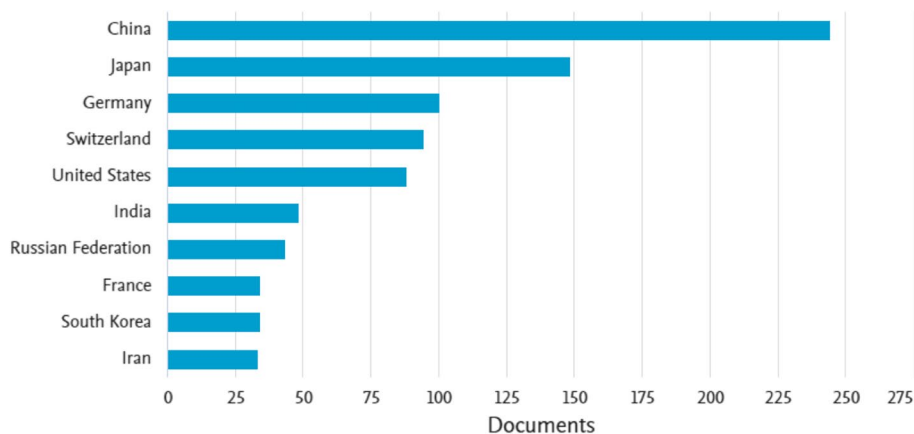


Fig. 3 Documents published by country (Reference: Scopus database)

Hosseini et al. 2019a) as well as its long-term sturdiness and consistency (Ke et al. 2023; Lee et al. 2013; Felice et al. 2023; Ghafoori et al. 2019; Xie et al. 2024) have already been studied and have given positive results. As a result, the Fe–Mn–Si SMAs would fit into the market for structural materials with the function of SME (Fig. 6).

Martensitic transformation

SMAs undergo a martensitic change in the forward phase. In general, they undergo a solid-state diffusionless transformation in which atoms travel in a regular pattern in relation to their surroundings. The parent phase is sheared uniformly, yielding a new crystal structure that has no changes in composition. Although the relative positions of atoms vary negligibly, the movement of atoms as a group can cause severe macroscopic deformations. A temperature shift, such as mechanical distortion or quenching can both cause the martensitic transition. A martensitic transformation that is induced mechanically occurs not just in shape memory alloys, but also in stainless steel, carbon steel, and a variety of other alloys. For instance, in the automotive industry, steels with high Mn (15–30% mass) are employed. They provide high strength and resistance to crashes for the body parts of the automobile because of their excellent ductility (with failure strains from 80 to 90%) and reasonably elevated ultimate strengths. The amount of Mn in these steels has a big impact on how they behave. As per the crystal structure, the typical Martensitic transformation in Fe-based alloys can be divided into two phases: transitions from the parent (FCC) to the martensite (BCC, BCT, or FCT) and transformations from parent to martensite (HCP). Fe–Mn–Si is by far the most exhaustively researched Fe-based SMA (Sato et al. 1982; Roca et al. 2017). Apart from the shape memory effect, Fe–Mn–Si has excellent fatigue performance and

is used as a seismic dampening component (Sawaguchi et al. 2016). The transition, however, is non-thermoelastic, thus not possible to attain superelasticity. It was reported that thermoelastic transformation can occur when a matrix is sufficiently reinforced and the BCT structure's tetragonality is sufficiently high (Maki et al. 1984; Maki n.d.). The transformation of the Fe–Ni–Co–Ti alloy to thermoelastic occurs because of the coherence of the phase's precipitation with the γ matrix (Maki et al. 1984). However, due to the brittleness generated by precipitation of grain boundary, it was previously not easy to achieve superelasticity at normal temperature (room temperature). This was solved by maintaining the character distribution of the grain boundary under control. Researchers have found the feasibility of superelasticity at normal temperature (room temperature) in Fe–Ni–Co–Al–Ta–B alloy in 2010 (Tanaka et al. 2010), and later the same property was found in its family of alloys, like Fe–Ni–Co–Al–Nb–B and Fe–Ni–Co–Al–Ti–B (Omori et al. 2013; Chumlyakov et al. 2016; Lee et al. 2014). In this work, the grain boundary energy was decreased with a strong recrystallization texture achieved through appropriate cold-rolling and annealing the result of which precipitation of the grain boundary was successfully inhibited. As a result, thin sheets can achieve a substantial super elastic strain of up to 13.5%; however, the brittleness of the wires remains because of the difficulties in attaining the low-energy grain boundary. In these alloy systems, γ parent phase's transformations to the martensitic phase are responsible for the characteristics of shape memory alloy. Fe–Mn–Al–Ni, a novel ferrous SMA was discovered in 2011 (Qiang et al. 2022). The crystal structures are portrayed in Fig. 7a and its superelasticity is portrayed in Fig. 7b. The microstructure of this alloy is comparable to that of Fe–Ni–Co-based SMAs.

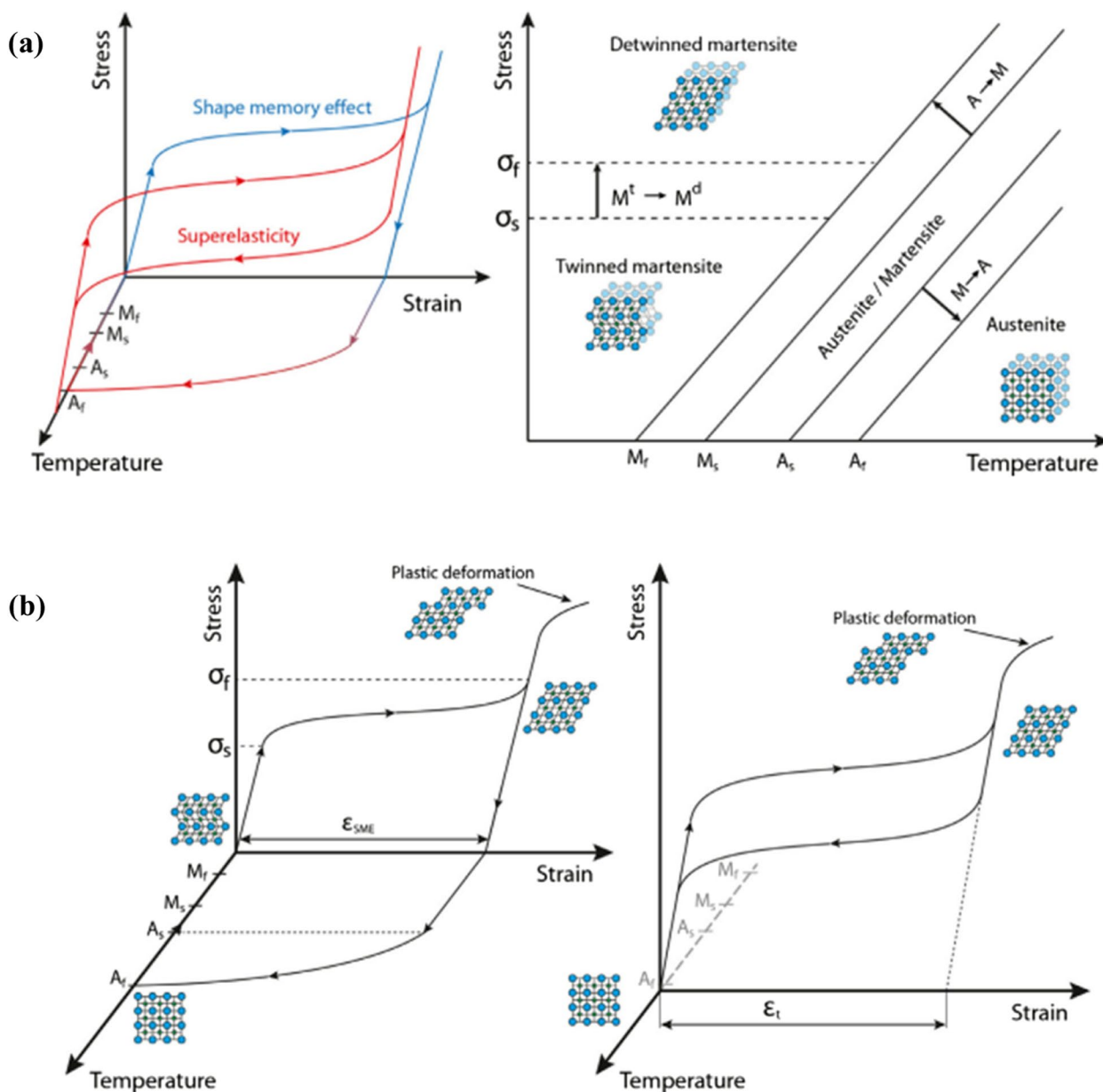


Fig. 4 a Picture depicting shape memory effect and superelasticity. b Stress strain temperature diagram and crystal lattices (Porentaa et al. 2021) (Reused from Elsevier under the Creative Commons CC-BY licence)

Furthermore, precipitates that are nanosized and coherent developed in a disordered matrix with an ordered structure proves vital in thermoelastic martensitic transition, despite the fact that the α (bcc) “ferrite” phase, transforms martensitically to γ (fcc) “austenite” phase, in contrast traditional Fe-based SMAs with γ parent phase. In the Fe–Mn–Ga system (Omori et al. 2009; Zhu et al. 2009), a comparable Martensitic transformation from the to the has been observed. The Fe–Mn–Al–Ni alloy can solve a problem in alloys that are

superelastic, which has large stress sensitivity to temperature for martensitic transformation and consequently small temperature window for superelasticity, as an addition to the merits of the cheap ingredients and appreciable ability towards cold working. Until now, superelasticity in Fe–Mn–Al–Ni alloy has been achieved at temperatures ranging from -263 to 240 °C, with a small dependence of the critical stress on the temperature; thus, this SMA is a promising material for practical applications. We can find further details about Fe–SMA alloys and strips in

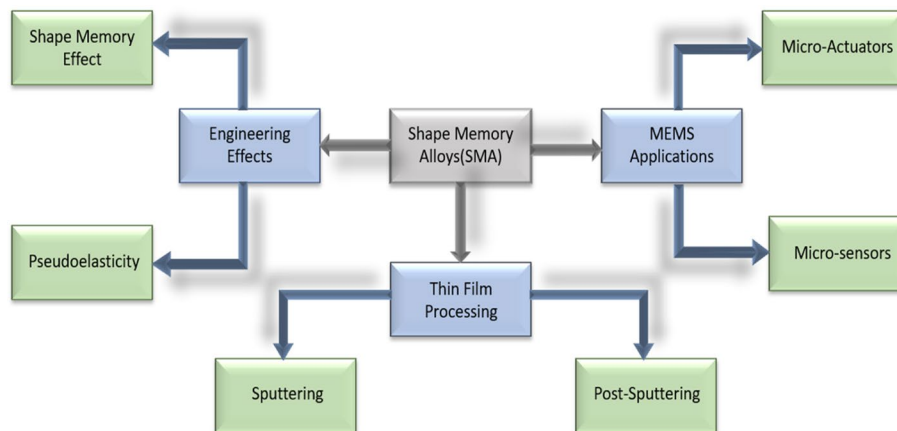


Fig. 5 General overview of SMAs

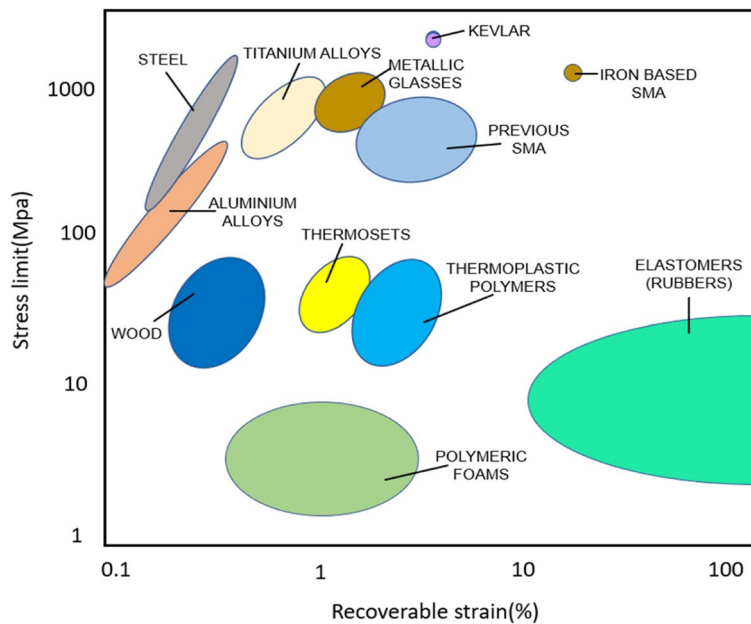


Fig. 6 Graph indicating the stress and recoverable strain of materials (Kanayo et al. 2016). The iron-based alloy referred here is Fe–28Ni–17Co–11.5Al–2.5Ta–0.05B (at.%); (reused with permission from Elsevier)

(Sawaguchi et al. 2016; Hosseini et al. 2019b; Soroushian et al. 1770). These Fe–SMA strips or rebars, are already in use and they can be found in a variety of rehabilitation projects (CEN 2004; Pan et al. 2019), and concrete T-beams that are shear-critical reinforced can be reinforced using Fe–SMA alloy.

Applications involving reinforced concrete beams

Shape memory alloys (SMAs) and already present or new RC bodies can be utilized together to give new capabilities or improve their protective ability and toughness,

according to recent research (Cladera et al. 2014a, 2014b; Fritsch et al. 2010; Abouali et al. 2019; Cortés-Puentes et al. 2018; Varughese and El-Hacha 2020). The majority of research on employing SMAs in structural engineering to date has focused on improving damping capacity and superelastic behavior by utilizing Ni–Ti alloys and Cu-based alloys, especially to develop vibration mitigation and enhance seismic resistance to civil structures (Cladera et al. 2014b; Cortés-Puentes et al. 2018; Varughese and El-Hacha 2020; Otsuka and Wayman 1998; Ozbulut et al. 2011a). However, one research has

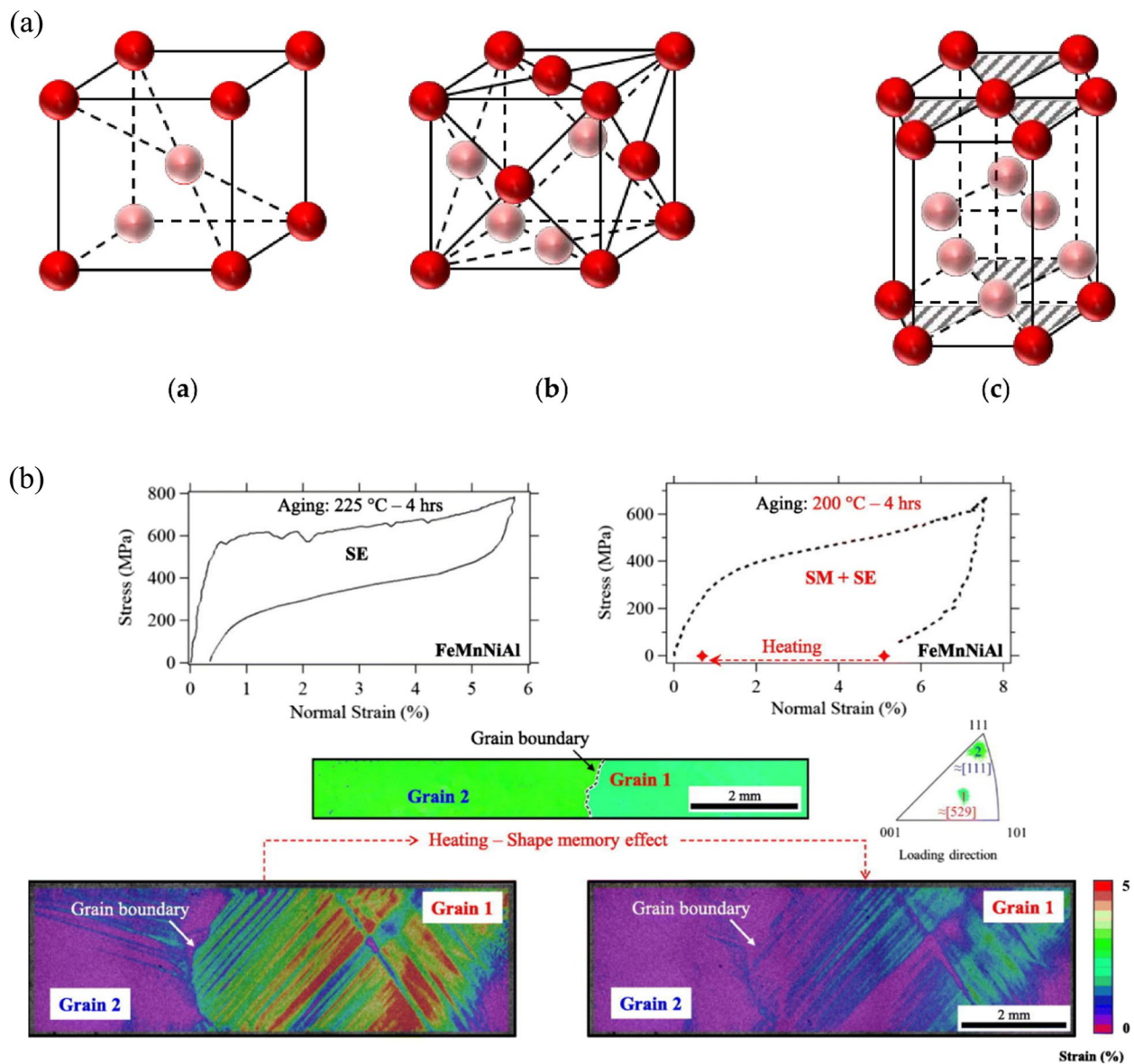


Fig. 7 a Crystal lattices of **a** α -Martensite (BCC); **b** γ -Austenite (FCC); **c** ϵ -Martensite (HCP). (Qiang et al. 2022) (Reused from MDPI under Creative Commons licence). **b** Superelasticity in Fe–Mn–Ni–Al SMA (Abuzaid and Sehitoglu 2019) (reused with permission from Elsevier)

employed superelastic behavior to develop the behavior of reinforced concrete members that are shear-critical and approaching their failure state. Mas et al. (2016) conducted experimental research on the shear failure of continuous rectangular spiral internal pseudoelastic Ni–Ti reinforced concrete beams. They came to the conclusion that trading steel reinforcement for SMAs in actual structure was hardly cost-effective due to current Ni–Ti's technology and price, and the fact that these materials should only be utilized in places of the structures where they are absolutely necessary because they permit the formation of high-tech fuses to safeguard the whole architecture.

As a result, studies to tackle the distinct structural challenges in specific places by using superelastic Ni–Ti alloys are still going strong (Nahar et al. 2019; Wang et al. 2019; Navarro-Gomez and Bonet 2019; Casagrande et al. 2019), and the same is happening in the study to use the other cost-effective SMAs like Cu–Al–Mn (Hosseini et al. 2019b). The research on utilizing Fe–SMA strips to retrofit reinforced concrete T-beams as shear external reinforcement was presented by Zerbe et al. (2017). The retrofitted beams' shear strength was increased by 20 to 25% in this study; however, the anchorage system used did influence the test results, and the final outcomes of

the research were hardly definitive. Montoya-Coronado et al. (2019) gave the latest findings of a campaign aimed at determining the possibility of utilizing Fe–SMA strips to reinforce shear critical beams using Fe–SMA strips through experiments. The Fe–SMA strips were thoroughly investigated. Ten small-scale beam tests clearly demonstrated the improvement in shear strength of beams that are retrofitted, by examining a fully wrapped new anchorage system. The findings of preliminary shear strengthening in T-beams were presented by Shahverdi et al. (2019). They utilized shotcrete mortar and ribbed “memory steel” stirrups. One significant discovery was that the system’s operation was not influenced by bending the corners of the stirrups. The prestressing effect was validated by reduced widths of crack for service loads, according to the authors who produced the results that a shotcrete layer embedded with Fe–SMA stirrups was a possible shear strengthening option which was straightforward for implementing in appropriate applications. The SMA employed in the shear strengthening procedures (Zerbe et al. 2017; Montoya-Coronado et al. 2019; Shahverdi et al. 2019) is a cost-effective SMA. The composition of the alloy is 63%Fe–17%Mn–5%Si–10%Cr–4%Ni–1% (V, C) (in mass %) (Dong et al. 2009). It’s worth noting that Fe, a relatively inexpensive mineral, makes up about 63 percent of its bulk. Despite the fact that superelasticity isn’t applicable for the mentioned alloy due to its imperfect martensitic transformation, the high ductility and shape memory effect (SME) are noticeable (Cladera et al. 2014a; Shahverdi et al. 2020; Hosseini et al. 2018) and contain extra information on Fe-based SMA alloys and strips. These Fe–SMA strips or rebars are being utilized in various projects involving real rehabilitation

(Schranz et al. 2019; Mercier et al. 2019), and they can be used to reinforce shear-critical concrete T-beams.

Other applications of Fe-based SMAs

Fe-based SMAs in civil engineering constructions are still in their infancy, with only a few research applications documented in the field. However, two uses in other similar industries have been successful: the fabrication of crane rail fishplates to link fixed sections of rails (as shown in Fig. 8), for highly durable cranes (Maruyama and Kubo 2011) and pipe couplings for pipelines. Ghafoori et al. investigated the alloy’s cyclic deformation and fatigue behavior (Izadia et al. 2018). They found that during high cycle fatigue loads, the stiffness of the alloy was fairly constant, but the recovery stress was reduced, which was attributed to transition-induced stress relief under fatigue loading. A formula was also proposed by them for safely designing alloys as structural reinforcement under high cycle fatigue loading conditions.

Moreover, Hosseini et al. investigated the development of stress recovery of alloys under various constraint parameters (Hosseini et al. 2018). They examined the pressure-treated alloy’s cyclic response after a second thermal activation. They discovered that, despite the fact that the amplitude of the restoring force decreased under cyclic loading, it was found that secondary thermal activation can recover most of the relaxed restoring force. Fe–SMAs are in the free-stressed austenite phase at ambient temperature. The stress causes a so-called martensitic transformation (i.e., direct transition) from γ austenite to ϵ martensite phase, producing stress-induced martensite. After heating and cooling, the recoverable martensitic phase transition can be reversed

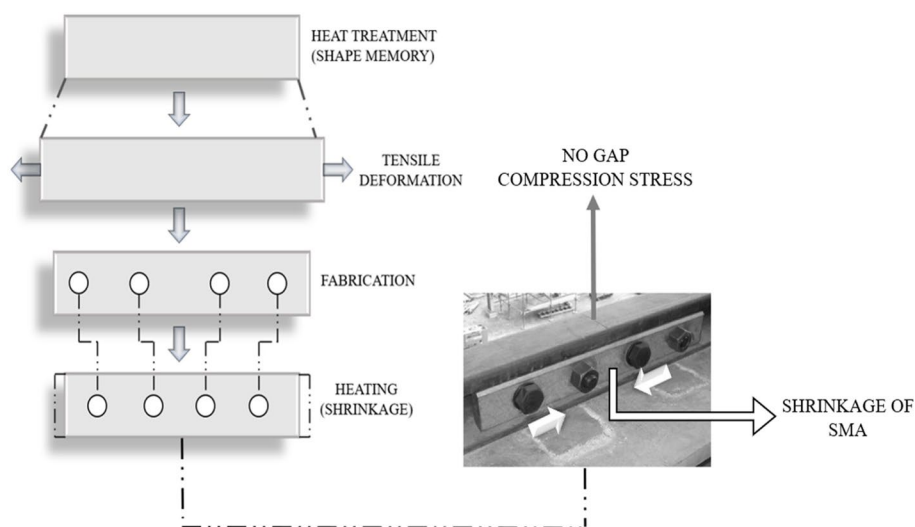


Fig. 8 Crane rail SMA fish-plate (schematic)

to form the austenitic phase. Consequently, during the reverse transformation, the Fe–SMA recovers its original shape. When the distortion of Fe–SMA is controlled while reverse transformation, the alloy creates restorative stresses in an attempt to come back to its original shape. This recovery stress could be applied to buildings to provide prestressing forces. Fe-based SMA strips were implanted in the center of the concrete bars and Fe-based SMA strips were also used to reinforce concrete beams (Czaderski et al. 2015). Fe–SMA ribbed reinforcement is

used in ongoing research to reinforce large beams. The key applications of Fe-based SMAs are listed in Fig. 9.

Transformation in Fe–Mn–Si–Cr–Ni SMA

The impact of microstructural changes on the shape memory performance of Fe15Mn7Si9Cr5Ni (wt.%) stainless steel SMA was reported by Bikas C et al. (2003). The transition temperatures and material composition of the component phases are given in Table 1.



Fig. 9 Applications of Fe-based SMAs

Table 1 Transformation temperatures of Fe–Mn–Si–Cr–Ni

Sample	M_s (Martensite start)	M_f (Martensite finish)	A_s (Austenite Start)	A_f (Austenite finish)	Composition (%)
A	24 °C	–26 °C	112 °C	171 °C	Fe: 63.42 Mn: 15.45 Si: 7.03 Cr: 9.11 Ni: 4.98
B	30 °C	–40 °C	122 °C	173 °C	Fe: 64.96 Mn: 14.51 Si: 7.27 Cr: 8.46 Ni: 4.81
C	24 °C	–31 °C	97 °C	173 °C	Fe: 64.44 Mn: 14.82 Si: 7.03 Cr: 8.87 Ni: 4.84

Transformation in Fe–Mn–Si–Co SMA

The transition temperatures of Fe–30Mn–6Si– x Co ($x=0$ to 9 wt. pct.) SMAs were investigated by Maji, B.C. et al. (2013). They came to the conclusion that adding cobalt lowers the hindrance to plastic yielding. The influence of (Fe, -Co)₅Mn₃Si₂ precipitates, however, induces an increase in flow stress above 5% Co. In Co-containing alloys, plastic yielding appears to be nonuniform and occurs concurrently with the formation of stress-induced martensite. Table 2 shows the transformation temperatures of Fe–Mn–Si–Co:

SME improvisation experiment in Fe–Mn–Si-based SMA

M.J. Xue et al. (2022). proposed decreasing annealing twin boundary (ATB) density to increase the shape memory effect of Fe–Mn–Si-based alloys. Their results showed that reducing ATB density does not result in the improvement of the shape memory effect. An ingot of the composition Fe–20Mn–5.5Si–9Cr–5Ni (wt%) was melted under an argon atmosphere using induction

melting. The cylindrical ingot was forged into a billet at 1050 °C. Blocks cut from the billet are subjected to a solution treatment, followed by water quenching. Certain blocks were annealed, followed by air cooling. The Shape memory effect of these samples was assessed by bending around a series of half-circle molds with different radii and performing tensile tests to analyze the strain and shape recovery. The TEM image of the alloy after 4% tensile deformation is shown in Fig. 10.

Experimental study of Fe–Mn–Si–Cr SMA

The cause of temperature's effect on critical stress of Fe–Mn–Si–Cr SMA for several loading conditions was inspected by Takamasa Yoshikawa et al. (2017). Fe–28Mn–6Si–5Cr is the chemical composition of the material utilized. This material's transition temperatures are listed below in Table 3.

The sample material rod was given a shape memory treatment at 1223 K for 30 min before being quenched in water. The material was initially loaded at varied temperatures. The pieces were loaded with tension,

Table 2 Transformation temperatures of Fe–Mn–Si–Co

Alloys	M_s (martensite start temperature)	M_f (martensite finish temperature)	A_s (austenite start temperature)	A_f (austenite finish temperature)
0 Co	59.58 °C	13.79 °C	134.39 °C	177.71 °C
1 Co	40.45 °C	–8.42 °C	131.48 °C	174.32 °C
3 Co	24.05 °C	–6.62 °C	133.57 °C	164.17 °C
5 Co	14.73 °C	–22.07 °C	130.76 °C	161.21 °C
7 Co	33.91 °C	–4.78 °C	134.04 °C	184.24 °C
9 Co	32.25 °C	–8.44 °C	135.56 °C	175.63 °C

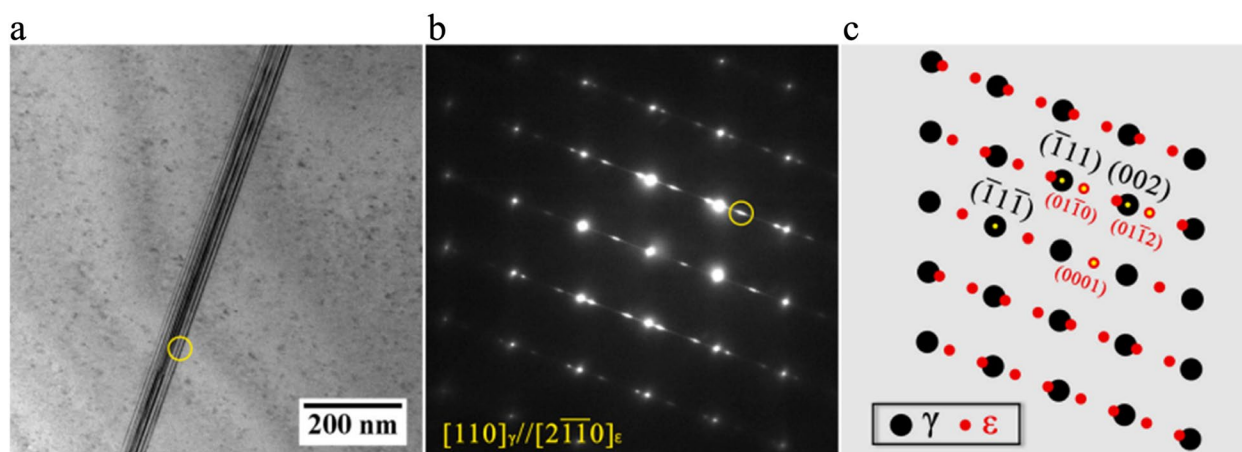


Fig. 10 TEM analysis after 4% tensile deformation. **a** Image portraying the stress-induced martensite plate. **b** Selected area diffraction pattern of the highlighted area. **c** Key figure of **b**. (Xue et al. 2022) (reused with permission from Elsevier)

Table 3 Transformation temperatures

M_s (Martensite start temperature)	M_f (Martensite finish temperature)	A_s (Austenite start temperature)	A_f (Austenite finish temperature)
29.1 °C	-3.8 °C	136.1 °C	167.7 °C

compression, and torsion at a strain rate of $2 \times 10^{-4} \text{ s}^{-1}$ under various temperatures. The high-temperature strain gauge was applied to calculate the strain as well as the shape recovery during sample loading and unloading. Experimental results show that this material undergoes a stress-induced martensitic transition before failure at ambient temperatures of uni-axial tension, compression, and torsion. Since the yield stress in that particular material is greater than martensitic transition stress at room temperature, it can exhibit a shape memory effect. Above 135 °C, the critical stresses of the materials change back. Rather than improving the SME of that material, deformation at temperatures above 135 °C improves the plastic workability. As a result, using the shape memory effect in that workpiece requires deformation below 135 °C.

A. Baruj et al. (2010) studied the mechanical behavior of Fe–28Mn–6Si–5Cr (wt%) alloy after basic thermomechanical treatment including aging at 800 °C for 10 min after rolling at 600 °C. They concluded that, up to 110 °C, martensite can be induced in this material and stress-induced martensite was not observed in this material at temperatures above 150 °C. Furthermore, at temperatures between 90 °C and 110 °C, a relatively substantial pseudo-elastic behavior was found, correlating with the fact that martensite occurs in this region.

J. Ma et al. (2012) used thermal cycling to study the shape memory properties of the single crystal material Fe–28Ni–17Co–11.5Al–2.5Ta (at. %) at constant levels of tensile and compressive stress. The observed transition strain levels in all samples were lower than theoretically evaluated, potentially due to a huge volume fraction of non-transforming particles, partial martensite alignment due to martensite variant interactions, and a marginally greater martensite c/a ratio in the specimens used in their research.

Iwamoto T. et al. (2015) performed an experimental analysis of the rate-sensitive tensile deformation characteristic of Fe–SMA alloys. Two separate test rigs were used to perform tensile tests on iron-based shape memory alloys at various strain rates: a current material testing machine and the split Hopkinson pressure bar technique-based impact testing equipment. During the testing, a thermocouple was used to record the temperature rise during quasi-static deformation. The improved deformation owing to the shape memory effect

was determined after a quasi-static test by heating the deformed specimen to the A_f temperature. At last, they conclude by making the following points:

1. The true stress level rises as the strain rates increase. The effect of positive rate sensitivity on deformation behavior may be seen clearly. The viscous drag that occurs during mobile dislocation and/or twinning causes stress to increase in proportion to the strain rate, which is a well-known thermal activation process. There is a correlation between the promotion of the deformation and an increase in temperature. A suppression of martensitic transformation is brought about as a result of the temperature change. A greater amount of stress should be applied due to the suppression in order to obtain the desired level of strain. Let us take a hypothetical scenario in which there is no heating as a result of irreversible work. This will help us better understand the mechanism. When the martensitic transformation itself becomes less significant in relation to the strain as a result of a change in the strain rate, the deformation process must be subjected to a significantly greater level of stress.
2. The shape recovery factor is independent of the strain rate for quasi-static tests using different strain rates. Figure 11 summarizes the effects of stress and temperature on the Fe–Mn–Si–Cr SMA.

Scope for applications and upcoming applications

Takahiro Sawaguchi et al. have worked on Fe–Mn–Si based Alloys to seismic response control (Sawaguchi et al. 2016). Wandong Wang et al. have developed a new approach for fatigue strengthening of structures made of metals that utilizes a property of SMA viz, shape memory effect of a Fe–SMA as well as the mechanism of bridging provided by the bonding process (Wang et al. 2021). Antoni Cladera et al. worked on using iron-based SMAs to reinforce slender concrete T-shaped beams (Cladera et al. 2020). T. Maruyama et al. have researched the connection of rails with SMA fishplates, SMA fishplates for crane rails, Pipe joints for steel pipes, and so on (Maruyama and Kubo 2011). Kinam Hong et al. Kinam Hong et al. wanted to see if a Fe–SMA might be used to reinforce civil structures (Hong et al. 2018). Diego Isidoro Heredia Rosa used uniaxial coupon experiments to explore the behavior of Fe–SMAs subjected to cyclic inelastic straining (Rosa et al. 2020). Mohammadreza Izadi et al. Retrofitted the steel bridge connections that are cracked due to fatigue using smart Fe–SMAs (Izadi et al. 2019a). Moslem Shahverdi et al. studied the material characterization of Fe-based SMA strips for the reinforcement of reinforced concrete components (Shahverdi et al. 2018). SMAs, such as Ni–Ti–Nb alloys, can be used

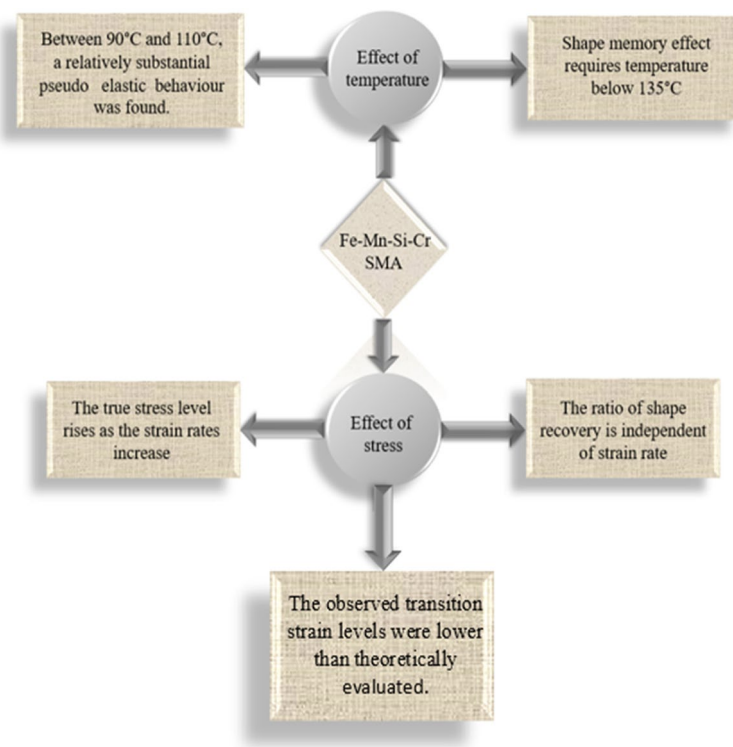


Fig. 11 Effect on Fe–Mn–Si–Cr SMA

in civil engineering applications because of their super-elasticity or SME properties (Choi et al. 2012; Wei and Xinqing 2009; Dommer and Andrawes 2012). In this area, some demonstration projects exist (Janke et al. 2005a; Indirli et al. 2001; Castellano et al. 2001; Moser et al. 2005; Shin and Andrawes 2010; Saiidi et al. 2007; Saiidi and Wang 2006). The SME feature of the shape memory alloys had been exploited before and after tensioning operations carried out in civil constructions (Janke et al. 2005a; Rojob and El-Hacha 2017), whereas energy dissipation and passive damping are the applications of superelasticity that have been primarily focused in civil engineering construction (Rojob and El-Hacha 2017; Sun and Rajapakse 2003; Graesser and Cozzarelli 1991). Conventional strengthening procedures can be addressed by the introduction of novel materials with unique features, like carbon-fiber reinforced polymers (CFRPs) and Fe-SMAs (Izadi et al. 2018a, 2018b; Hollaway 2002; Teng et al. 2012; Ghafoori and Motavalli 2015a; Ghafoori et al. 2012). The usage of prestressed (activated) CFRP composites for fatigue strengthening of various steel members has piqued curiosity (Teng et al. 2012; Ghafoori et al. 2012; Ghafoori and Motavalli 2015b, 2015c; Shaat et al. 2004), but the usage of prestressed Fe-SMAs for steel strengthening is a relatively new concept (Izadi et al. 2018a, 2018b; Izadi et al. 2019b) and has a greater scope

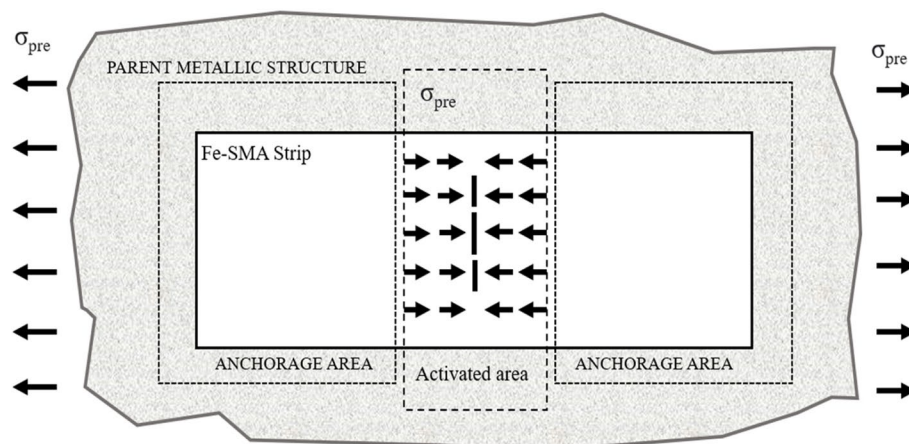
for future applications and research. Table 4 lists the current research on iron-based SMAs in the field of civil engineering.

Current research needs

Despite extensive investigations on the behavior of Fe–Mn–Si alloys, some aspects remain unsolved, necessitating future research on specific topics. Despite the fact that the recovery stresses are an essential crucial place for employing SMAs as prestressing materials, a vast majority of studies on thermomechanical treatments throughout the process of production have concentrated on something like developing the recovery strain, etc. As a result, a thorough examination of improving the efficiency of recovery stresses for various compositions of alloys is necessary. Furthermore, relaxation and fatigue aspects have not been adequately explored in terms of material attributes. More information on corrosion behavior can be found, but for prestressing applications, knowing the corrosion characteristics of concrete in an alkaline environment is essential. Obtaining huge amounts of materials that are necessary for civil engineering applications and extremely large production demands research. In order to produce any product, it is a necessity to develop weldability expertise. Various publications cover the weldability characteristics in the

Table 4 Applications in civil structures

Composition	Application	Reference
Fe–20.2Mn–5.6Si–8.9Cr–5.0Ni	Control of Seismic response.	Sawaguchi et al. 2016)
Fe–17Mn–5Si–10Cr–4Ni–1(V, C)	A new approach for fatigue strengthening of structures made of metals that utilizes a property of SMA viz, SME of a Fe–SMA as well as the mechanism of bridging provided by the bonding process. (as shown in Fig. 12)	Wang et al. 2021)
Fe–17Mn–5Si–10Cr–4Ni–1(V, C)	Reinforce slender concrete T-shaped beams.	Cladera et al. 2020)
Fe–17Mn–5Si–10Cr–4Ni–1(V, C)	Reinforce civil structures.	Hong et al. 2018)
Fe–Mn–Si–Cr–Ni	Performed uniaxial coupon experiments to explore the characteristics of (Fe–SMAs) subjected to inelastic cyclic straining.	Rosa 2020)
Fe–Mn–Si–Cr–Ni	Retrofitted the steel bridge connections that are cracked due to fatigue using smart Fe–SMAs.	Izadi et al. 2019a)
Fe–17Mn–5Si–10Cr–4Ni–1(V, C)	Material characterization of Fe–SMA strips for the reinforcement of RC components.	Shahverdi et al. 2018)
Fe–17Mn–5Si–10Cr–5Ni	Seismic damping application.	Fang et al. 2021)
Fe–17Mn–5Si–10Cr–4Ni–1(V, C)	The cyclic behavior of activated SMA after a second thermal activation was investigated in this study.	Hosseini et al. 2018)
Fe–Mn–Si–Cr–Ni	This was the first study to look at the structural fire behavior of structural members strengthened by prestressed Fe–SMA in a systematic way.	Ghafoori et al. 2019)
Fe–17Mn–5Si–10Cr–4Ni–1(V, C)	The Fe–Mn–Si–Cr–Ni SMA fatigue behavior and cyclic deformation were investigated.	Ghafoori et al. 2017)
Fe–17Mn–5Si–10Cr–4Ni–1(V, C)	They investigated how Fe–SMA strips strengthened and prestressed RC beams.	Shahverdi et al. 2016)
Fe–27.2Mn–5.69Si–5.02Cr–0.047C	They inferred that, with increasing levels of pretensile strain, the bending strength of the Fe–Mn–Si–Cr SMA composites increases.	Watanabe et al. 2002)
Fe–16Mn–5Si–10Cr–4Ni–1(V, N)	According to the findings, pre-deformation at room temperature prior to aging or deformation at lower temperature after aging process can increase shape memory qualities greatly.	Li et al. 2013)

**Fig. 12** Novel fatigue strengthening method done by Wandong Wang et al. (2021) (Reused from Elsevier under the terms of the Creative Commons CC-BY license)

austenite phase of Fe-based SMAs, however for a given welded alloy kept in the martensitic phase, knowing the temperature-influenced zone in it for various welding procedures would be immensely beneficial. The development of low-cost materials and the research of novel industrial applications for Fe-based SMAs are the two main issues to be tackled. Given that the Fe–Mn–Si SMA shows only one cycle of the SME and afterward functions

as a reinforcement component at the installation site, we are optimistic about establishing a new application field for it. The Fe–Mn–Al–Ni SMA also suffers from cyclic superelasticity deterioration, which is a common problem with superelastic alloys. In Fe–Mn–Al–Ni alloys, rapid superelasticity deterioration has been observed (Vollmer et al. 2016), which should be addressed for realistic cyclic applications. Long-term aging at room

temperature has also been found to change the critical stress (Ozcan et al. 2018). The temperature-based SME has received less study because the output stress values that are received as output are not found to be significant. The reverse SME (Peng et al. 2017) was just observed. Due to its best-in-class shape memory capabilities (Miyazaki et al. 1981, 1999) and biocompatibility (Mantovani 2000), Ni–Ti alloys are being commercially used in sectors such as healthcare, automobile, aviation, and seismic, as well as for end-user goods (Humbeeck 1999; Morgan 2004; Jani et al. 2014; Desroches and Smith 2004; Janke et al. 2005b). No real application of Fe-based SMAs for structural damping has been documented so far. The large damping impact generated by the martensitic transformation is reported in TRIP/TWIP Fe–Mn alloys (Lee et al. 1996; Jee et al. 1997; Frommeyer et al. 2003; Watanabe et al. 2010). Sawaguchi et al. (Sawaguchi et al. 2006a, 2006b) discovered that the Fe–28Mn–6Si–5Cr–05NbC SMAs had a damping capacity of over 0.1% in the large-strain amplitude area. The corrosion resistance of Fe–Mn–Si SMAs has been investigated for various compositions of alloys in severe surroundings like NaCl and H₂SO₄ solutions (Söderberg et al. 1999; Lin et al. 2002; Huang et al. 2004; Maji et al. 2006; Hu et al. 2009; Charfi et al. 2009, 2012; Della Rovere et al. 2011, 2012a, 2012b). The corrosion resistance in an alkaline environment, however, is yet to be investigated. Although several investigations on the weldability features of Fe-based SMAs have been conducted (Janke et al. 2005a; Lin et al. 2000; Dong et al. 2006; Qiao et al. 2007; Zhou et al. 2010, 2012), more research is required. Some other

SMAs, like Ni–Ti or Cu–based alloys, are being used in structural applications (Li et al. 2013; Alam et al. 2007; Song et al. 2006; Czaderski et al. 2006; Wu et al. 2012; Ozbulut et al. 2011b; Sun 2011; Branco et al. 2012; Isalgue et al. 2012; Dommer and Andrawes 2012; Muntasir-Billah and Alam 2012; Cladera et al. 2013; Torra et al. 2013), therefore Fe-based SMAs should receive more attention for their construction applications. However, as the demand for SMAs develops, researchers must concentrate their efforts on creating new SMAs with new capabilities and features (Fe-based SMAs), which will be a viable replacement for Ni–Ti SMAs in the near future. Figure 13 summarises the key research needed to pursue research in the field of Fe-based SMAs. Figure 13 summarises the key research needed to pursue research in the field of Fe-based SMAs.

Conclusions

This paper gives an overview of the Martensitic transformation of different compositions of Fe-based SMAs, their applications, and future research needs. In comparison with original alloys that emerged in the 1980s, study on new Fe-based SMAs has accelerated significantly in the last decade, with the development of Fe–Mn–Si alloys which yield recovery stresses at a higher level at reduced temperature conditions. Utilization of Fe-based SMA tendons for replacing or reinforcing actual buildings is propitious for the foreseeable future. There are various advantages to using iron-based SMA tendons, including negligible friction losses, no need for anchor heads and ducts, and no need for room to apply the force by

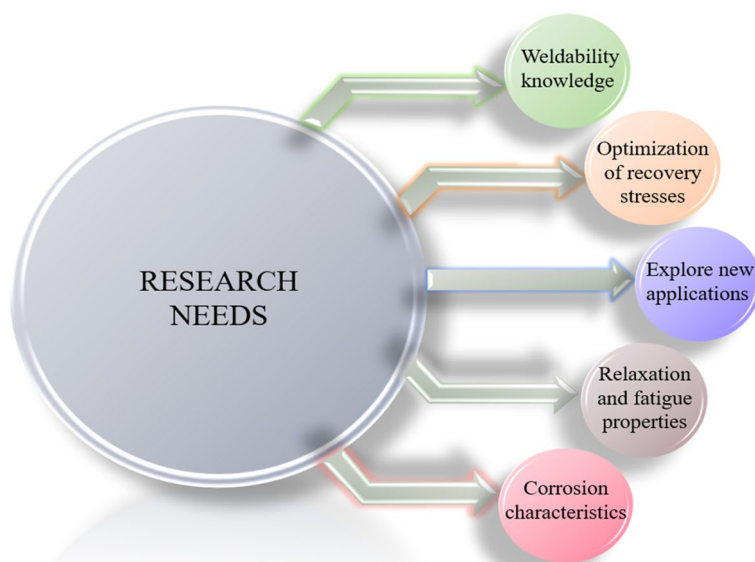


Fig. 13 Current research needs

hydraulic equipment. The cost has been cheaper for these new Fe-based SMAs because of the usage of inexpensive iron as well as the ability to melt and produce those SMAs in regular atmospheric conditions. These novel Fe–Mn–Si alloys have stronger elastic stiffness and broad temperature transition hysteresis than existing SMAs, such as Ni–Ti alloys. They are also easy to work with, corrosion-resistant, and weldable. In recent times, new Fe–Mn–Si shape memory alloys that have fine precipitates are being produced, conceding for high recovery stresses without requiring thermomechanical conditioning.

Acknowledgements

Not applicable

Authors' contributions

The authors confirm their contribution to the paper as follows: study conception and design: S.S.; data collection: P.M.; analysis and interpretation of results: S.S., P.M.; draft manuscript preparation: S.S. All authors reviewed the results and approved the final version of the manuscript.

Funding

One of the authors, Dr Santosh Sampath gratefully acknowledges the funding from Science and Engineering Research Board (SERB), India and Sri Sivasubramaniya Nadar Trust through file numbers, SUR/2022/001060 and SSN/IFFP/DECEMBER 2021/1–21/08, respectively.

Availability of data and materials

Since this is a review paper there is no data associated with the manuscript.

Declarations

Competing interests

The authors declare that they have no competing interests.

Received: 7 April 2024 Accepted: 3 July 2024

Published online: 14 July 2024

References

- Abouali S, Shahverdi M, Ghassemieh M, Motavalli M (2019) Nonlinear simulation of reinforced concrete beams retrofitted by near-surface mounted iron-based shape memory alloys. *Eng Struct* 189:133–148. <https://doi.org/10.1016/j.engstruct.2019.02.060>
- Abuzaid W, Sehitoglu H (2019) Shape memory effect in Fe–Mn–Ni–Al iron-based shape memory alloy. *Scr Mater* 169:57–60. <https://doi.org/10.1016/j.scriptamat.2019.05.006>
- Alam MS, Youssef MA, Nehdi M (2007) Utilizing shape memory alloys to enhance the performance and safety of civil infrastructure: a review. *Can J Civil Eng* 34:1075–1086. <https://doi.org/10.1139/07-038>
- Baruj A, Bertolino G, Troiani HE (2010) Temperature dependence of critical stress and pseudoelasticity in a Fe–Mn–Si–Cr pre-rolled alloy. *J Alloy Compd* 502:54–58. <https://doi.org/10.1016/j.jallcom.2010.04.123>
- Branco M, Guerreiro L, Mahesh KK, Braz Fernandes FM (2012) Effect of load cycling on the phase transformations in Ni–Ti wires for civil engineering applications. *Constr Build Mater* 36:508–519. <https://doi.org/10.1016/j.conbuildmat.2012.06.003>
- Casagrande L, Sisinni J, Bonati A, Occhiuzzi A, Auricchio F (2019) Integrated shape memory alloy devices toward a high-performance glazed curtain wall seismic retrofit. *Eng Struct* 179:540–555. <https://doi.org/10.1016/j.engstruct.2018.11.023>
- Castellano MG, Indirli M, Martelli A (2001) Progress of application, research and development and design guidelines for Shape Memory Alloy devices for cultural heritage structures in Italy, Proceedings of SPIE - The International Society for Optical Engineering. 250–261. <https://doi.org/10.1117/12.434124>
- CEN (2004) EC2 Design of concrete structures. Part 1: General rules and rules for buildings. European Committee for Standardization (CEN), Brussels
- Charfi A, Bouraoui T, Feki M, Bradai C, Normand B (2009) Surface treatment and corrosion behaviour of Fe–32Mn–6Si shape memory alloy. *C R Chim* 12:270–275. <https://doi.org/10.1016/j.crci.2007.11.008>
- Charfi A, Gamaoun F, Bouraoui T, Bradai C, Normand B (2012) Shape memory effect improvement and study of the corrosion resistance of the Fe–8Mn–6Si–13Cr–6Ni–12Co alloy. *Adv Mater Res* 476–478:2162–2170. <https://doi.org/10.4028/www.scientific.net/AMR.476-478.2162>
- Choi E, Nam TH, Chung YS, Kim YW, Lee SY (2012) Behaviour of NiTiNb SMA wires under recovery stress or prestressing. *Nanoscale Res Lett* 7:1–11. <https://doi.org/10.1186/1556-276X-7-66>
- Chumlyakov YI, Kireeva IV, Kuts OA, Platonova YN, Poklonov VV, Kukshauzen IV, Kukshauzen DA, Panchenko MY, Reunova KA (2016) Thermoelastic martensitic transformations in single crystals of FeNiCoAlX(B) alloys. *Russ Phys J* 58:1549–1556. <https://doi.org/10.1007/s40830-017-0129-9>
- Cladera A, Weber B, Leinenbach C, Czaderski C, Shahverdi M, Motavalli M (2014a) Iron based shape memory alloys for civil engineering structures: an overview. *Constr Build Mater* 63:281–293. <https://doi.org/10.1016/j.conbuildmat.2014.04.032>
- Cladera A, Montoya-Coronado LA, Ruiz-Pinilla JG, Ribas C (2020) Shear strengthening of slender reinforced concrete T-shaped beams using iron-based shape memory alloy strips. *Eng Struct* 221:111018. <https://doi.org/10.1016/j.engstruct.2020.11.1018>
- Cladera A, Oller E, Ribas C (2013) Pilot experiences in application of shape memory alloys in structural concrete. *J Mater Civ Eng.* (in press). [https://doi.org/10.1061/\(ASCE\)MT.1943-5533.0000974](https://doi.org/10.1061/(ASCE)MT.1943-5533.0000974)
- Cladera A, Oller E, Ribas C (2014) Pilot experiences in the application of shape memory alloys in structural concrete. *J Mater Civ Eng* 26. [https://doi.org/10.1061/\(ASCE\)MT.1943-5533.0000974](https://doi.org/10.1061/(ASCE)MT.1943-5533.0000974)
- Cortés-Puentes L, Zaidi M, Palermo D, Dragomirescu E (2018) Cyclic loading testing of repaired SMA and steel reinforced concrete shear walls. *Eng Struct* 168:128–141. <https://doi.org/10.1016/j.engstruct.2018.04.044>
- Czaderski C, Hahnebach B, Motavalli M (2006) RC beam with variable stiffness and strength. *Constr Build Mater* 20:824–833. <https://doi.org/10.1016/j.conbuildmat.2005.01.038>
- Czaderski C, Weber B, Shahverdi M, Motavalli M (2015) Iron-based shape memory alloys (Fe-SMA) - a new material for prestressing concrete structures. *SMAR 2015 - 3rd Conference on Smart Monitoring, Assessment and Rehabilitation of Structure*
- Della Rovere CA, Alano JH, Otubo J, Kuri SE (2011) Corrosion behavior of shape memory stainless steel in acid media. *J Alloys Compd* 509:5376–5380. <https://doi.org/10.1016/j.jallcom.2011.02.051>
- Della Rovere CA, Alano JH, Silva R, Nascente PAP, Otubo J, Kuri SE (2012a) Characterization of passive films on shape memory stainless steels. *Corros Sci* 57:154–161. <https://doi.org/10.1016/j.corsci.2011.12.022>
- Della Rovere CA, Alano JH, Silva R, Nascente PAP, Otubo J, Kuri SE (2012b) Influence of alloying elements on the corrosion properties of shape memory stainless steels. *Mater Chem Phys* 133:668–673. <https://doi.org/10.1016/j.matchemphys.2012.01.049>
- Desroches R, Smith B (2004) Shape memory alloys in seismic resistant design and retrofit: a critical review of their potential and limitations. *J Earthq Eng* 8:415–429. <https://doi.org/10.1080/13632460409350495>
- Dommer K, Andrawes B (2012) Thermomechanical characterization of NiTiNb shape memory alloy for concrete active confinement applications. *J Mater Civ Eng* 24:1274–1282. [https://doi.org/10.1061/\(ASCE\)MT.1943-5533.0000495](https://doi.org/10.1061/(ASCE)MT.1943-5533.0000495)
- Dommer K, Andrawes B (2012) Thermomechanical characterization of NiTiNb shape memory alloy for concrete active confinement applications. *J Mater Civ Eng* 24:1274–82.1292. [https://doi.org/10.1061/\(ASCE\)MT.1943-5533.0000495](https://doi.org/10.1061/(ASCE)MT.1943-5533.0000495)
- Dong ZZ, Sawaguchi T, Kajiwara S, Kikuchi T, Kim SH, Lee GC (2006) Microstructure change and shape memory characteristics in welded Fe–28Mn–6Si–5Cr–0.53Nb–0.06C alloy. *Mater Sci Eng A*. 438–440:800–803. <https://doi.org/10.1016/j.msea.2005.12.054>
- Dong Z, Klotz UE, Leinenbach C, Bergamini A, Czaderski C, Motavalli M (2009) A novel Fe–Mn–Si shape memory alloy with improved shape recovery properties by VC precipitation. *Adv Eng Mater* 11:40–44. <https://doi.org/10.1002/adem.200800312>

- Evirgen A, Ma J, Karaman I, Luoa ZP, Chumlyakov YI (2012) Effect of aging on the superelastic response of a single crystalline FeNiCoAlTa shape memory alloy. *Scripta Mater.* 67:475–478. <https://doi.org/10.1016/j.scriptamat.2012.06.006>
- Fang C, Wang W, Ji Y, Yam MCH (2021) Superior low-cycle fatigue performance of iron-based SMA for seismic damping application. *J Constr Steel Res* 184:106817. <https://doi.org/10.1016/j.jcsr.2021.106817>
- Felice IO, Shen J, Barragan AFC, Moura IAB, Li B, Wang B, Khodaverdi H, Mohri M, Schell N, Ghafoori E, Santos TG, Oliveira JP (2023) Wire and arc additive manufacturing of Fe-based shape memory alloys: Microstructure, mechanical and functional behavior. *Mater Design* 231:112004. <https://doi.org/10.1016/j.matdes.2023.112004>
- Fritsch E, Izadi M, Ghafoori E (2010) Development of nail-anchor strengthening system with iron-based shape memory alloy (Fe-SMA) strips. *Constr Build Mater* 229:117042. <https://doi.org/10.1016/j.conbuildmat.2019.117042>
- Frommeyer G, Brück U, Neumann P (2003) Supra-ductile and high-strength manganese-TRIP/TWIP steels for high energy absorption purposes. *ISIJ Int* 43:438–446. <https://doi.org/10.2355/isijinternational.43.438>
- Ghafoori E, Motavalli M (2015a) Normal, high and ultra-high modulus carbon fiber-reinforced polymer laminates for bonded and un-bonded strengthening of steel beams. *Mater Des* 67:232–243. <https://doi.org/10.1016/j.matdes.2014.11.031>
- Ghafoori E, Motavalli M (2015b) Lateral-torsional buckling of steel I-beams retrofitted by bonded and un-bonded CFRP laminates with different pre-stress levels: experimental and numerical study. *Constr Build Mater* 76:194–206. <https://doi.org/10.1016/j.conbuildmat.2014.11.070>
- Ghafoori E, Motavalli M, Botsis J, Herwig A, Galli M (2012) Fatigue strengthening of damaged metallic beams using prestressed unbonded and bonded CFRP plates. *Int J Fatigue* 44:303–315. <https://doi.org/10.1016/j.ijfatigue.2012.03.006>
- Ghafoori E, Hosseini E, Leinenbach C, Michels J, Motavalli M (2017) Fatigue behavior of a Fe-Mn-Si shape memory alloy used for prestressed strengthening. *Mater Design.* <https://doi.org/10.1016/j.matdes.2017.07.055>
- Ghafoori E, Neuenschwander M, Shahverdi M, Czaderski C, Fontana M (2019) Elevated temperature behaviour of an iron-based shape memory alloy used for prestressed strengthening of civil structures. *Constr Build Mater* 211:437–452. <https://doi.org/10.1016/j.conbuildmat.2019.03.098>
- Ghafoori E, Motavalli M (2015) Innovative CFRP-Prestressing system for strengthening metallic structures. *J Compos Constr* 19. [https://doi.org/10.1061/\(ASCE\)CC.1943-5614.0000559](https://doi.org/10.1061/(ASCE)CC.1943-5614.0000559)
- Graesser EJ, Cozzarelli FA (1991) Shape-memory alloys as new materials for aseismic isolation. *J Eng Mech* 117:2590–2608. [https://doi.org/10.1061/\(ASCE\)0733-9399\(1991\)117:11\(2590\)](https://doi.org/10.1061/(ASCE)0733-9399(1991)117:11(2590))
- Hollaway LC, Cadei J (2002) Progress in the technique of upgrading metallic structures with advanced polymer composites. *Prog Struct Eng Mat.* 4:131–148. <https://doi.org/10.1002/pse.112>
- Hong K, Lee S, Han S, Yeon Y (2018) Evaluation of Fe-based shape memory alloy (Fe-SMA) as strengthening material for reinforced concrete structures. *Appl Sci* 8:730. <https://doi.org/10.3390/app8050730>
- Hosseini E, Ghafoori E, Leinenbach C, Motavalli M, Holdsworth SR (2018) Stress recovery and cyclic behaviour of an Fe-Mn-Si shape memory alloy after multiple thermal activation. *Smart Mater Struct* 27:025009. <https://doi.org/10.1088/1361-665X/aaa2c9>
- Hosseini A, Michels J, Izadi MR, Ghafoori E (2019a) A comparative study between Fe-SMA and CFRP reinforcements for prestressed strengthening of metallic structures. *Constr Build Mater* 226:976–992. <https://doi.org/10.1016/j.conbuildmat.2019.07.169>
- Hosseini F, Gencturk B, Jain A, Shahzade K (2019b) Optimal design of bridge columns constructed with engineered cementitious composites and Cu-Al-Mn superelastic alloys. *Eng Struct* 198:109531. <https://doi.org/10.1016/j.engstruct.2019.109531>
- Hu BQ, Bai PK, Dong ZZ, Cheng J (2009) Effect of Cu addition on corrosion resistance and shape memory effect of Fe-14Mn-5Si-9Cr-5Ni alloy. *T Nonferr Metal Soc* 19:149–153. [https://doi.org/10.1016/S1003-6326\(08\)60243-5](https://doi.org/10.1016/S1003-6326(08)60243-5)
- Huang X, Chen S, Hsu TY, Zuyao XU (2004) Corrosion behavior of Fe₂₅Mn-6Si₅Cr shape memory alloys modified with rare earth in a NaCl solution. *J Mater Sci* 39:6857–6859. <https://doi.org/10.1023/B:JMSS.0000045620.49206.6a>
- Indirli M, Castellano MG, Clemente P, Martelli A (2001) Demo-application of Shape Memory Alloy devices: the rehabilitation of the S. Giorgio Church Bell-Tower. *SPIE Smart Systems for Bridges, Structures, and Highways.* pp 262–272
- Isalgue A, Auguet C, Carreras G, Torra V (2012) SMA (Cu-Based, NiTi) for use in damping: the implications of reliability for long time applications and aging behavior. *Funct Mater Lett* 5:1250008. <https://doi.org/10.1142/S1793604712500087>
- Iwamoto T, Fujita K (2015) An experimental study on rate-sensitive tensile deformation behaviour of Fe-based shape memory alloy. *Mater Web of Conf* 33(04003):1–6. [https://doi.org/10.1051/mateconf/20153304003\(conference\)](https://doi.org/10.1051/mateconf/20153304003(conference))
- Izadi MR, Ghafoori E, Motavalli M, Maalek S (2018) Iron-based shape memory alloy for the fatigue strengthening of cracked steel plates: effects of re-activations and loading frequencies. *Eng Struct.* 176:953–967. <https://doi.org/10.1016/j.engstruct.2018.09.021>
- Izadi MR, Ghafoori E, Shahverdi M, Motavalli M, Maalek S (2018) Development of an iron-based shape memory alloy (Fe-SMA) strengthening system for steel plates. *Eng Struct.* 174:433–446. <https://doi.org/10.1016/j.engstruct.2018.07.073>
- Izadi M, Motavalli M, Ghafoori E (2019a) Iron-based shape memory alloy (Fe-SMA) for fatigue strengthening of cracked steel bridge connections. *Constr Build Mater* 227:116800. <https://doi.org/10.1016/j.conbuildmat.2019.116800>
- Izadi M, Ghafoori E, Hosseini A, Michels J, Motavalli M (2019b) Thermally activated iron-based shape memory alloy for strengthening metallic girders. *Thin Wall Struct* 141:389–401. <https://doi.org/10.1016/j.tws.2019.04.036>
- Izadia MR, Ghafoori E, Shahverdi M, Motavalli MB, Maalek S (2018) Development of an iron-based shape memory alloy (Fe-SMA) strengthening system for steel plates. *Eng Struct* 174:433–446. <https://doi.org/10.1016/j.engstruct.2018.07.073>
- Jani JM, Leary M, Subic A, Gibson MA (2014) A review of shape memory alloy research, applications and opportunities. *Mater Design* 56:1078–1113. <https://doi.org/10.1016/j.matdes.2013.11.084>
- Janke L, Czaderski C, Motavalli M, Ruth J (2005a) Applications of shape memory alloys in civil engineering structures – overview, limits and new ideas. *Mater Struct* 38:578–592. <https://doi.org/10.1007/BF02479550>
- Janke L, Czaderski C, Motavalli M, Ruth J (2005b) Applications of shape memory alloys in civil engineering structures - overview, limits and new ideas. *Mater Struct* 38:578–592. <https://doi.org/10.1007/BF02479550>
- Jee KK, Jang WY, Baik SH, Shin MC, Choi CS (1997) Damping capacity in Fe-Mn based alloys. *Scripta Mater* 37:943–948. [https://doi.org/10.1016/S1359-6462\(97\)00198-X](https://doi.org/10.1016/S1359-6462(97)00198-X)
- Kanayo K, Eloho A, Okotete A (2016) Reconciling viability and cost-effective shape memory alloy options – a review of copper and iron-based shape memory metallic systems. *Eng Sci Technol Int J* 19:1582–1592. <https://doi.org/10.1016/j.jestch.2016.05.010>
- Ke W, Yan W, Oliveira JP, Pang B, Chen L, Wu Y, Teshome FB, Shen J, Wang L, Tan C, Peng B, Song X, Zeng Z (2023) Thermal-fluid behavior, microstructure and mechanical properties in liquid bridge transfer mode during directed energy deposition-arc additive manufacturing – Insights using NiTi as a model alloy. *Addit Manuf* 77:103807. <https://doi.org/10.1016/j.addma.2023.103807>
- La Roca P, Baruj A, Sade M (2017) Shape-memory effect and pseudoelasticity in Fe-Mn-based alloys. *Shape Mem Superelast* 3:37–48. <https://doi.org/10.1007/s40830-016-0097-5>
- Lee YK, Jun JH, Choi CS (1996) Effect of ϵ martensite content on the damping capacity of Fe-17%Mn alloy. *Scripta Mater* 35:825–830. [https://doi.org/10.1016/S1359-6462\(96\)00231-X](https://doi.org/10.1016/S1359-6462(96)00231-X)
- Lee WJ, Weber B, Feltrin G, Czaderski C, Motavalli M, Leinenbach C (2013) Stress recovery behaviour of an Fe-Mn-Si-Cr-Ni-VC shape memory alloy used for prestressing. *Smart Mater Struct* 22:125037. <https://doi.org/10.1088/0964-1726/22/12/125037>
- Lee D, Omori T, Kainuma R (2014) Ductility enhancement and superelasticity in Fe-Ni-Co-Al-Ti-B polycrystalline alloy. *J Alloy Compd* 617:120–123. <https://doi.org/10.1016/j.jallcom.2014.07.136>
- Lee WJ, Partovi-Nia R, Suter T, Leinenbach C (2016) Electrochemical characterization and corrosion behaviour of an Fe-Mn-Si shape memory alloy in simulated concrete pore solutions. *Mater Corros* 67:839–846. <https://doi.org/10.1002/maco.201508701>

- Li K, Dong Z, Liu Y, Zhang L (2013) A newly developed Fe-based shape memory alloy suitable for smart civil engineering. *Smart Mater Struct* 22:045002. <https://doi.org/10.1088/0964-1726/22/4/045002>
- Lin HC, Lin KM, Chuang YC, Chou TS (2000) Welding characteristics of Fe–30Mn–6Si and Fe–30Mn–6Si–5Cr shape memory alloys. *J Alloys Compd* 306:186–192. [https://doi.org/10.1016/S0925-8388\(00\)00762-3](https://doi.org/10.1016/S0925-8388(00)00762-3)
- Lin HC, Lin KM, Lin CS, Ouyang TM (2002) The corrosion behavior of Fe-based shape memory alloys. *Corros Sci* 44:2013–2026. [https://doi.org/10.1016/S0010-938X\(02\)00027-6](https://doi.org/10.1016/S0010-938X(02)00027-6)
- Maji BC, Krishnan M (2003) The effect of microstructure on the shape recovery of a Fe–Mn–Si–Cr–Ni stainless steel shape memory alloy. *Scr Mater* 48:71–77. [https://doi.org/10.1016/S1359-6462\(02\)00348-2](https://doi.org/10.1016/S1359-6462(02)00348-2)
- Maji BC, Das CM, Krishnan M, Ray RK (2006) The corrosion behaviour of Fe–15Mn–7Si–9Cr–5Ni shape memory alloy. *Corros Sci* 48:937–949. <https://doi.org/10.1016/j.corsci.2005.02.024>
- Maji BC, Krishnan M, Sujata M, Ray RK (2013) Effect of Co addition on the microstructure, martensitic transformation and shape memory behaviour of Fe–Mn–Si alloys. *Metall Mater Trans A* 44:172–185. <https://doi.org/10.1007/s11661-012-1378-z>
- Maki T, Kobayashi K, Minato M, Tamura I (1984) Thermoelastic martensite in an ausedged Fe–Ni–Ti–Co alloy. *Scr Metall* 18:1105–1109. [https://doi.org/10.1016/0036-9748\(84\)90187-X](https://doi.org/10.1016/0036-9748(84)90187-X)
- Maki T (n.d.) Ferrous shape memory alloys. In: Otsuka K, Wayman CM (eds) *Shape memory materials*. Cambridge University Press, Cambridge, pp 117–132
- Mantovani D (2000) Shape memory alloys: properties and biomedical applications. *J Miner Met Mater Soc* 52:36–44. <https://doi.org/10.1007/s11837-000-0082-4>
- Maruyama T, Kubo H (2011) Ferrous (Fe-based) shape memory alloys (SMAs): properties, processing and applications, *Shape Memory and Superelastic Alloys Applications and Technologies*: 141–159. <https://doi.org/10.1533/9780857092625.2.141>
- Mas B, Cladera A, Ribas C (2016) Experimental study on concrete beams reinforced with pseudoelastic Ni–Ti continuous rectangular spiral reinforcement failing in shear. *Eng Struct* 127:759–768. <https://doi.org/10.1016/j.engstruct.2016.09.022>
- Mercier J, Basile B, Hallopeau X, Michels J, Tourneur C (2019) Structural concrete strengthening with fe-sma strips: case study with specific control after activation, *SMAR 2019 - Fifth Conf. Smart Monit. Assess. Rehabil. Civ. Struct., Zurich, Switzerland*
- Michels J, Shahverdi M, Czaderski C, El-Hacha R (2018) Mechanical performance of iron-based shape-memory alloy ribbed bars for concrete prestressing. *ACI Mater J*. 115:877–886. https://doi.org/10.14359/51710_959
- Miyazaki S, Otsuka K, Suzuki Y (1981) Transformation pseudoelasticity and deformation-behaviour in a Ti–50.6at-percent Ni alloy. *Scripta Metall Mater* 15:287–292. [https://doi.org/10.1016/0036-9748\(81\)90346-X](https://doi.org/10.1016/0036-9748(81)90346-X)
- Miyazaki S, Mizukoshi K, Ueki T, Sakuma T, Liu Y (1999) Fatigue life of Ti–50 at.% Ni and Ti–40Ni–10Cu (at.%) shape memory alloy wires. *Mater Sci Eng A* 273:658–663. [https://doi.org/10.1016/S0921-5093\(99\)00344-5](https://doi.org/10.1016/S0921-5093(99)00344-5)
- Montoya-Coronado LA, Ruiz-Pinilla JG, Ribas C, Cladera A (2019) Experimental study on shear strengthening of shear critical RC beams using iron-based shape memory alloy strips. *Eng Struct* 200:109680. <https://doi.org/10.1016/j.engstruct.2019.109680>
- Morgan NB (2004) Medical shape memory alloy applications—the market and its products. *Mater Sci Eng A* 378:16–23. <https://doi.org/10.1016/j.msea.2003.10.326>
- Moser K, Bergamini A, Christen R, Czaderski C (2005) Feasibility of concrete prestressed by shape memory alloy short fibers. *Mater Struct* 38:593–600. <https://doi.org/10.1007/BF02479551>
- Muntasir-Billah AHM, Alam SM (2012) Seismic performance of concrete columns reinforced with hybrid shape memory alloy (SMA) and fiber reinforced polymer (FRP) bars. *Constr Build Mater* 28:730–742. <https://doi.org/10.1016/j.conbuildmat.2011.10.020>
- Nahar M, Muntasir Billah AHM, Kamal HR, Islam K (2019) Numerical seismic performance evaluation of concrete beam-column joint reinforced with different super elastic shape memory alloy rebars. *Eng Struct*. 194:161–172. <https://doi.org/10.1016/j.engstruct.2019.05.054>
- Navarro-Gomez A, Bonet JL (2019) Improving the seismic behaviour of reinforced concrete moment resisting frames by means of SMA bars and ultra-high-performance concrete. *Eng Struct* 197:109409. <https://doi.org/10.1016/j.engstruct.2019.109409>
- Omori T, Watanabe K, Umetsu RY, Kainuma R, Ishida K (2009) Martensitic transformation and magnetic field-induced strain in Fe–Mn–Ga shape memory alloy. *Appl Phys Lett* 95:082508. <https://doi.org/10.1063/1.3213353>
- Omori T, Abe S, Tanaka Y, Lee DY, Ishida K, Kainuma R (2013) Thermoelastic martensitic transformation and superelasticity in Fe–Ni–Co–Al–Nb–B polycrystalline alloy. *Scr Mater* 69:812–815. <https://doi.org/10.1007/s40830-017-0129-9>
- Otsuka K, Wayman CM (1998) *Shape memory materials*. Cambridge University Press, United Kingdom
- Ozbulut OE, Hurlbeaus S, Desroches R (2011a) Seismic response control using shape memory alloys: a review. *J Intell Mater Syst Struct* 22:1531–1549. <https://doi.org/10.1177/1045389X11411220>
- Ozbulut OE, Hurlbeaus S, Desroches R (2011b) Seismic response control using shape memory alloys: a review. *J Intel Mat Syst Struct* 22:1531–1549. <https://doi.org/10.1177/1045389X11411220>
- Ozcan H, Ma J, Karaman I, Chumlyakov YI, Santamarta R, Brown J, Noebe RD (2018) Microstructural design considerations in Fe–Mn–Al–Ni shape memory alloy wires: effects of natural aging. *Scr Mater* 142:153–157. <https://doi.org/10.1016/j.scriptamat.2017.07.033>
- Pan S, Hu M, Zhang X, Hui H, Wang S (2019) A new near-surface-mounted anchorage system of shape memory alloys for local strengthening. *Smart Mater Struct* 28:025016. <https://doi.org/10.1088/1361-665X/aaf24e>
- Peng HB, Huang P, Zhou TN, Wang SL, Wen YH (2017) Reverse shape memory effect related to alpha, gamma transformation in a Fe–Mn–Al–Ni shape memory alloy. *Metall Mater Trans A* 48A:2132–2139. <https://doi.org/10.1007/s11661-017-3991-3>
- Porentaa L, Lavrencic M, Dujc J, Brojana M, Tušek J, Brank B (2021) Modeling large deformations of thin-walled SMA structures by shell finite elements. *Commun Nonlinear Sci Numer Simul* 101:105897. <https://doi.org/10.1016/j.cnsns.2021.105897>
- Qiang X, Chen L, Jiang X (2022) Achievements and perspectives on Fe-based shape memory alloys for rehabilitation of reinforced concrete bridges: an overview. *Materials* 15:8089
- Qiao Z, Li L, Wang D, Li Z (2007) Microstructure and shape recovery characteristics in a TiG-welded Fe–Mn–Si–Cr–Ni shape memory alloy. *Proc SPIE Int Soc Opt Eng* 6423:64233O. <https://doi.org/10.1117/12.779667>
- Rojob H, El-Hacha R (2017) Self-prestressing using iron-based shape memory alloy for flexural strengthening of reinforced concrete beams. *ACI Struct J* 114:523. <https://doi.org/10.14359/51689455>
- Rosa DH, Hartloper A, e Sousa ADC, Lignos DG, Motavalli M, Ghafoori E (2020) Experimental behaviour of iron-based shape memory alloys under cyclic loading histories. *Constr Build Mater* 272:121712. <https://doi.org/10.1016/j.conbuildmat.2020.121712>
- Saiidi MS, Sadrossadat-Zadeh M, Ayoub C, Itani A (2007) Pilot study of behaviour of concrete beams reinforced with shape memory alloys. *J Mater Civ Eng* 19:454–461. [https://doi.org/10.1061/\(ASCE\)0899-1561\(2007\)19:6\(454\)](https://doi.org/10.1061/(ASCE)0899-1561(2007)19:6(454))
- Saiidi MS, Wang HY (2006) Exploratory study of seismic response of concrete columns with shape memory alloys reinforcement. *ACI Struct J*. 103:435–442
- Sato A, Chishima E, Soma K, Mori T (1982) Shape memory effect in gamma reversible epsilon transformation in Fe–30mn–1si alloy single-crystals. *Acta Metall Mater* 30:1177–1183. [https://doi.org/10.1016/0001-6160\(82\)90011-6](https://doi.org/10.1016/0001-6160(82)90011-6)
- Sawaguchi T, Kikuchi T, Ogawa K, Yin F, Kajiwara S, Kushibe A et al (2006a) Internal friction of Fe–Mn–Si-based shape memory alloys containing Nb and C and their application as a seismic damping material. *Key Eng Mat* 319:53–58. <https://doi.org/10.4028/www.scientific.net/KEM.319.53>
- Sawaguchi T, Sahu P, Kikuchi T, Ogawa K, Kajiwara S, Kushibe A, Higashino M, Ogawa T (2006b) Vibration mitigation by the reversible fcc/hcp martensitic transformation during cyclic tension–compression loading of an Fe–Mn–Si-based shape memory alloy. *Scripta Mater* 54:1885–1890. <https://doi.org/10.1016/j.scriptamat.2006.02.013>
- Sawaguchi T, Maruyama T, Otsuka H, Kushibe A, Inoue Y, Tsuzaki K (2016) Design concept and applications of Fe–Mn–Sibased alloys -from shape-memory to seismic response control. *Mater Trans* 57:283–293. <https://doi.org/10.2320/matertrans.MB201510>

- Sawaguchi T, Maruyama T, Otsuka H, Kushibe A, Inoue Y, Tsuzaki K (2016) Design concept and applications of Fe-Mn-Si-based alloys from shape-memory to seismic response control. *Mater Trans.* 57:283–293. <https://doi.org/10.2320/matertrans.MB201510>
- Schranz B, Michels J, Shahverdi M, Czaderski C (2019) Strengthening of concrete structures with iron-based shape memory alloy elements: Case studies. SMAR 2019 - Fifth Conf. Smart Monit. Assess. Rehabil. Civ. Struct., Zurich, Switzerland
- Shaht A, Schnerch D, Fam A, Rizkalla S (2004) Retrofit of steel structures using fiber reinforced polymers (FRP): State-of-the-art. Transportation research board (TRB) annual meeting
- Shahverdi M, Czaderski C, Motavalli M (2016) Iron-based shape memory alloys for prestressed near-surface mounted strengthening of reinforced concrete beams. *Constr Build Mater* 112:28–38. <https://doi.org/10.1016/j.conbuildmat.2016.02.174>
- Shahverdi M, Michels J, Czaderski C, Motavalli M (2018) Iron-based shape memory alloy strips for strengthening RC members: Material behaviour and characterization. *Constr Build Mater* 173:586–599. <https://doi.org/10.1016/j.conbuildmat.2018.04.057>
- Shahverdi M, Czaderski C, Michels J (2019) 'Memory steel' for shear reinforcement of concrete structures. SMAR 2019 - Fifth Conf. Smart Monit. Assess. Rehabil. Civ. Struct., Potsdam. <https://www.dora.lib4ri.ch/empa/islandora/object/empa%3A19790>
- Shahverdi M, Michels J, Czaderski C, Motavalli M. Iron-based shape memory alloy strips for strengthening RC members: material behaviour and characterization. A. Cladera, et al. *Engineering Structures* 221 (2020) 111018 13 *Constr Build Mater* 2018;173:586–99. <https://doi.org/10.1016/j.conbuildmat.2018.04.057>
- Shin M, Andrawes B (2010) Experimental investigation of actively confined concrete using shape memory alloys. *Eng Struct* 32:656–664. <https://doi.org/10.1016/j.engstruct.2009.11.012>
- Söderberg O, Liu XW, Yakovenko PG, Ullakko K, Lindroos VK (1999) Corrosion behaviour of Fe–Mn–Si based shape memory steels trained by cold rolling. *Mater Sci Eng A* 273–275:543–548. [https://doi.org/10.1016/S0921-5093\(99\)00396-2](https://doi.org/10.1016/S0921-5093(99)00396-2)
- Song G, Ma N, Li HN (2006) Applications of shape memory alloys in civil structures. *Eng Struct* 28:1266–1274. <https://doi.org/10.1016/j.engstruct.2005.12.010>
- Soroushian P, Ostowari K, Nossoni A, Chowdhury H (2001) Repair and strengthening of concrete structures through application of corrective post-tensioning forces with shape memory alloys. *Transp Res Rec.* 1770:20–26. <https://doi.org/10.3141/1770-03>
- Sun W (2011) Seismic response control of high arch dams including contraction joint using nonlinear super-elastic SMA damper. *Constr Build Mater* 25:3762–3767. <https://doi.org/10.1016/j.conbuildmat.2011.04.013>
- Sun S, Rajapakse RKND (2003) Dynamic response of a frame with SMA bracing. *Proceedings of SPIE*, vol 5053. SPIE, San Diego, pp 262–270
- Tanaka Y, Himuro Y, Kainuma R, Sutou Y, Omori T, Ishida K (2010) Ferrous polycrystalline shape-memory alloy showing huge superelasticity. *Science* 327:1488–1490. <https://doi.org/10.1126/science.1183169>
- Teng JG, Yu T, Fernando D (2012) Strengthening of steel structures with fiber-reinforced polymer composites. *J Constr Steel Res.* 78:131–143. <https://doi.org/10.1016/j.jcsr.2012.06.011>
- Torra V, Auguet C, Isalgue A, Carreras G, Terriault P, Lovey FC (2013) Built in dampers for stayed cables in bridges via SMA. The SMARTER-ESF project: a mesoscopic and macroscopic experimental analysis with numerical simulations. *Eng Struct.* 49:43–57. <https://doi.org/10.1016/j.engstruct.2012.11.011>
- Van Humbeeck J (1999) Non-medical applications of shape memory alloys. *Mater Sci Eng A* 273:134–148. [https://doi.org/10.1016/S0921-5093\(99\)00293-2](https://doi.org/10.1016/S0921-5093(99)00293-2)
- Varughese K, El-Hacha R (2020) Design and behaviour of steel braced frame reinforced with NiTi SMA wires. *Eng Struct* 212:110502. <https://doi.org/10.1016/j.engstruct.2020.110502>
- Vollmer M, Krooss P, Kriegel MJ, Klemm V, Somsen C, Ozcan H, Karaman I, Weidner A, Rafaja D, Biermann H, Niendorf T (2016) Cyclic degradation in bamboo-like Fe–Mn–Al–Ni shape memory alloys — The role of grain orientation. *Scr Mater* 114:156–160. <https://doi.org/10.1016/j.scripamat.2015.12.007>
- Wang JQ, Li S, Hedayati Dezfuli F, Alam MS (2019) Sensitivity analysis and multicriteria optimization of SMA cable restrainers for longitudinal seismic protection of isolated simply supported highway bridges. *Eng Struct* 189:509–522. <https://doi.org/10.1016/j.engstruct.2019.03.091>
- Wang W, Li L, Hosseini A, Ghafoori E (2021) Novel fatigue strengthening solution for metallic structures using adhesively bonded Fe-SMA strips: a proof of concept study. *Int J Fatigue* 148:106237. <https://doi.org/10.3929/ethz-b-000477355>
- Watanabe Y, Miyazaki E, Okada H (2002) Enhanced mechanical properties of Fe–Mn–Si–Cr shape memory fiber/plaster smart composite. *Mater Trans* 43:974–983. <https://doi.org/10.2320/matertrans.43.974>
- Watanabe Y, Sato H, Nishino Y, Kim T (2010) Training effects on damping capacity in Fe–Mn and Fe–Mn–Cr alloys. *Mater Sci Forum* 638–642:2201–2206. <https://doi.org/10.1016%2Fj.msea.2008.01.038>
- Wei L, Xinqing Z (2009) Mechanical properties and transformation behaviour of NiTiNb shape memory alloys. *Chin J Aeronaut* 22:540–543. [https://doi.org/10.1016/S1000-9361\(08\)60138-7](https://doi.org/10.1016/S1000-9361(08)60138-7)
- Wu M, Johannesson B, Geiker M (2012) A review: self-healing in cementitious materials and engineered cementitious composite as a self-healing material. *Constr Build Mater* 28:571–583. <https://doi.org/10.1016/j.conbuildmat.2011.08.086>
- Xie J, Chen Y, Wang H, Zhang T, Zheng M, Wang S, Yin L, Shen J, Oliveira JP (2024) Phase transformation mechanisms of NiTi shape memory alloy during electromagnetic pulse welding of Al/NiTi dissimilar joints. *Mater Sci Eng A* 893:146119. <https://doi.org/10.1016/j.msea.2024.146119>
- Xue MJ, Xue XY, Zhang H, Li JS, Lai MJ (2022) Re-examination of the effect of reducing annealing twin boundary density on the shape memory effect in Fe–Mn–Si-based alloys. *J Alloys Compd* 907:164505. <https://doi.org/10.1016/j.jallcom.2022.164505>
- Yoshikawa T, Inaba T, Ida K, Mizutani S (2017) Experimental study of critical stresses of Fe–28Mn–6Si–5Cr SMA under various temperature conditions. *Advances in Shape Memory Materials*, 221–229. https://doi.org/10.1007/978-3-319-53306-3_17
- Zerbe L, Reda M, Dawood M, Belarbi A, Senouci A, Gencturk B et al (2017) Behaviour of retrofitted concrete members using iron-based shape memory alloys. SMAR 2017 - Fourth Conf. Smart Monit. Assessment Rehabil. Civ. Struct., Zurich
- Zhou C, Lin C, Liu L (2010) Study on YAG laser welding process of Fe–Mn–Si shape memory alloy. *Appl Mech Mater* 37–38:1364–1367. <https://doi.org/10.4028/www.scientific.net/AMM.37-38.1364>
- Zhou C, Lin C, Liu L (2012) Study on CO2 laser weldability of Fe–Mn–Si shape memory alloy. *Proc SPIE Int Soc Opt Eng* 8409. <https://doi.org/10.1117/12.921518>
- Zhu W, Liu EK, Feng L, Tang XD, Chen JL, Wu GH, Liu HY, Meng FB, Luo HZ (2009) Magnetic-field-induced transformation in FeMnGa alloys. *Appl Phys Lett* 95:222512. <https://doi.org/10.1063/1.3269590>

Publisher's Note

Springer Nature remains neutral with regard to jurisdictional claims in published maps and institutional affiliations.